Electronic Supplementary Material (ESI) for CrystEngComm.

Electronic Supplementary Information

Controlling crystal growth of potassium iodide with 1,1´-bis(pyridin-4-ylmethyl)-2,2´-biimidazole ligand (L) – formation of linear $[K_4I_4L_4]_n$ polymer with cubic $[K_4I_4]$ core units

Margarita Bulatova, Rajendhraprasad Tatikonda, Pipsa Hirva, Evgeny Bulatov, Elina Sievänen, Matti Haukka

Abstract: Crystal growth of potassium iodide was controlled by using neutral organic (1,1'-bis(pyridin-4-ylmethyl)-2,2'-biimidazole (further L) ligand as the modifier. Selected modifier allows to maintain original cubic $[K_4I_4]$ units and arrange them into a linear ligand-supported 1D chain. The supported $[K_4I_4]$ cubes are only slightly distorted compared to the cubes found in pure KI salt. The N-K binding of the ligand to the KI salt, as well as weak I···H, N···H, and N···I interactions stabilize the structure to create a unique 1D polymer of neutral potassium iodide ionic salt inside the $[K_4I_4L_4]_n$ complex.

Table of Contents

Synthetic procedures

Synthesis of 1,1'-bis(pyridin-4-ylmethyl)-2,2'-biimidazole ligand

1,1'-bis(pyridin-4-ylmethyl)-2,2'-biimidazole (further ligand or L) was synthesized according to the procedure described in the literature,[1] with slight modifications: 4-(bromomethyl)pyridine*HBr was used as a starting material (**Scheme S1**), the resulted product was purified on the silica 60 column and recrystallized from methanol to give colorless product. Yield: 317.9 mg (52.8 %).

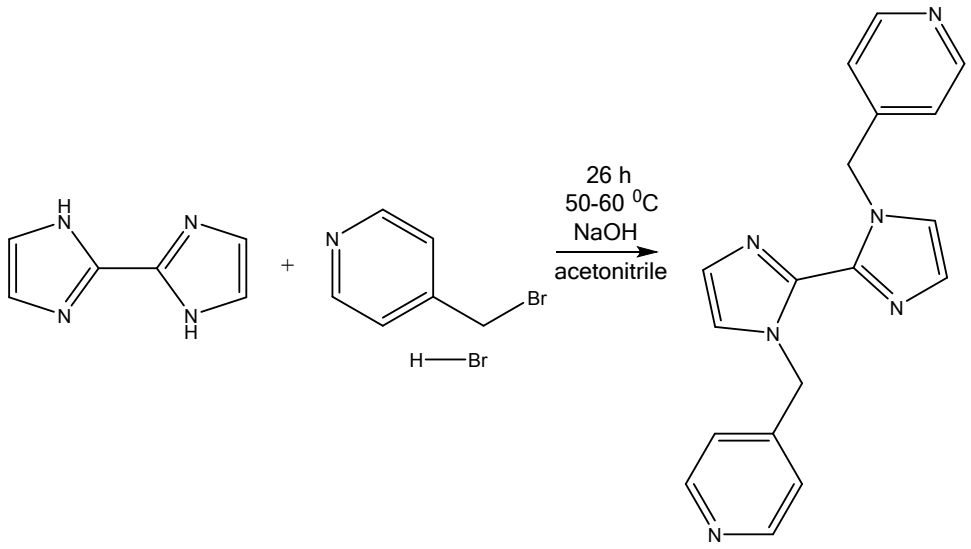

Scheme S1. Synthesis of the ligand.

Synthesis of a 1D polymeric $[K_4I_4L_4]_n$ chain

KI (0.3 mmol, 49.8 mg) and 1,1'-bis(pyridin-4-ylmethyl)-2,2'-biimidazole (0.1 mmol, 31.6 mg) were dissolved in 0.6 ml of MeOH in a glass vial. Mixture was stirred for 10 min at RT and left for crystallization by slow evaporation (**Scheme S2**). Colorless crystals of $[K_4I_4L_4]_n$ were obtained after 4 days in a yield of 34.4 mg (71.4 %) and characterized by EA, SCXRD, PXRD and NMR.

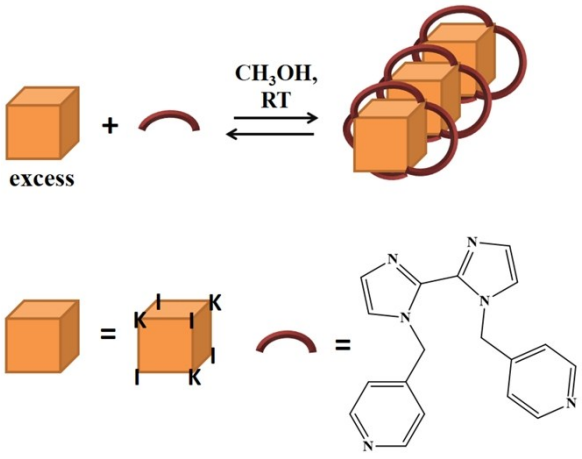

Scheme S2. Reaction of L and KI to obtain a polymeric $[K_4I_4L_4]_n$ chain.

Solid state studies

Ligand coordination to KI was studied in solid state both for single crystal and for the bulk material.

Single crystal X-ray analysis (SCXRD). Experimental Procedures

The crystals of $[K_4I_4L_4]_n$ were immersed in cryo-oil, mounted in a MiTeGen loop, and measured at 123 K on a Rigaku Oxford Diffraction Supernova diffractometer using Cu Kα radiation. The *CrysAlisPro*[2] program package was used for cell refinement and data reduction. Multi-scan absorption correction (*CrysAlisPro*[2]) was applied to the intensities before structure solution. The structures were solved by charge flipping method using the *SUPERFLIP*[3] software. Structural refinements were carried out using *SHELXL-2014*.[4] All H-atoms were positioned geometrically and constrained to ride on their parent atoms, with C-H = 0.95-0.99 Å and $U_{iso} = 1.2 \cdot U_{eq}$ (parent atom).

Single crystal X-ray analysis (SCXRD). Crystallographic Details

Crystallographic details are summarized in **Table S1.** Discussion of the structure can be found in original paper.

Table S1. Crystal Data.

	KIL
empirical formula	$C_{18}H_{16}IKN_6$
fw	482.37
temp (K)	123(2)
λ(Å)	1.54184
cryst syst	Tetragonal
space group	$P4_2/n$
a (Å)	23.56060(19)
b (Å)	23.56060(19)
c (Å)	6.92267(8)
V (Å^3)	3842.79(8)
Z	8
ρ_{calc} (Mg/m^3)	1.668
μ(Kα) (mm^{-1})	15.149
No. reflns.	18332
Unique reflns.	4035
GOOF (F^2)	1.059
R_{int}	0.0336
R1[a] ($I \geq 2\sigma$)	0.0262
wR2[b] ($I \geq 2\sigma$)	0.0670

[a] $R1 = \Sigma||F_o| - |F_c||/\Sigma|F_o|$; [b] $wR2 = [\Sigma[w(F_o^2 - F_c^2)^2]/ \Sigma[w(F_o^2)^2]]^{1/2}$.

NMR spectroscopy. Experimental Procedures

^{15}N CPMAS NMR spectra of the solid state samples were recorded at room temperature with Bruker Avance 400 MHz spectrometer equipped with a CPMAS probe, using 4 mm ZrO_2 rotors. The samples were spun at a rate of 10 kHz, the CP contact time being 3 ms and the relaxation delay 5 s. The ^{15}N chemical shifts were calibrated using nitrogen signal of a glycine sample at 33.4 ppm (with respect of liquid NH_3 at 0 ppm) as an external standard.

NMR spectroscopy. Results and Discussion

^{15}N CPMAS NMR spectroscopy was used to investigate complexation of the potassium ion with the ligand in the solid state. Two magnetically non-equivalent nitrogen nuclei resonating at chemical shift values of δ = 200.09 ppm and δ = 251.82 ppm corresponding to the pyridine and biimidazole nitrogen atoms respectively were revealed (**Figure S1**). The difference between chemical shift values of both biimidazole nitrogen atoms in solid state ^{15}N NMR is insignificant and they both resonate at the same 200.09 ppm value. In case of complex only one magnetically non-equivalent nitrogen nuclei resonating at chemical shift value of δ = 199.09 ppm was observed (**Figure S2**). Disappearing of pyridine ^{15}N chemical shifts can be explained by coordination of pyridine nitrogen atoms to KI in the bulk material, and therefore, quenching the ^{15}N pyridine signal.

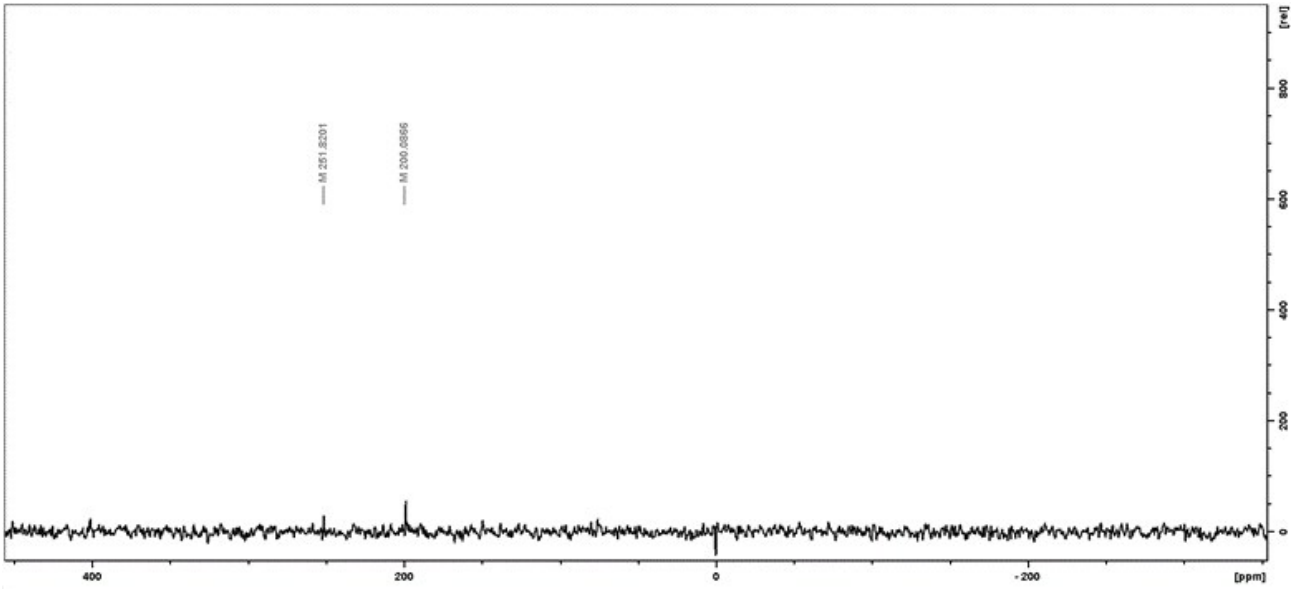

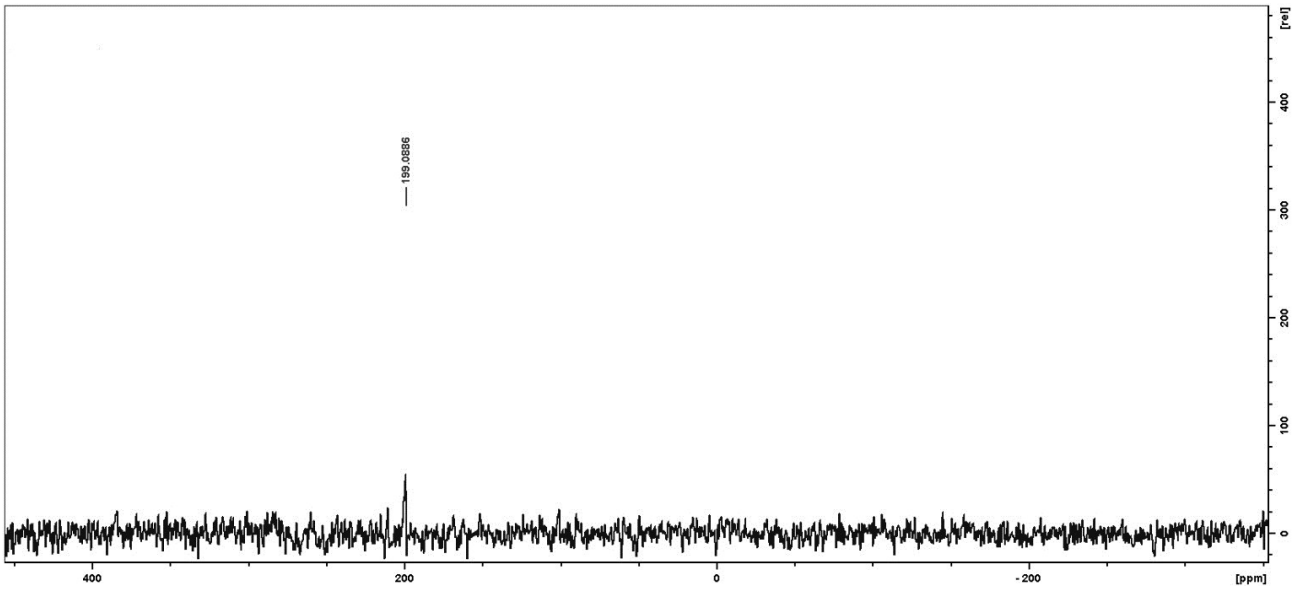

Figure S1. Solid state ^{15}N CPMAS NMR spectrum of the ligand.

Figure S2. Solid state ^{15}N CPMAS NMR spectrum $[K_4I_4L_4]_n$.

Luminescence spectroscopy. Experimental Procedures

Luminescence spectra in solid state were recorded using Varian Cary Eclipse Fluorescence Spectrophotometer. Grinded powder samples were pressed into the thin layer between quartz plates and fixed in fluorimeter at slightly different from 45° angle to the incident beam.

Luminescence spectroscopy. Results and Discussion

The organic ligand L in pure form is luminescent in solid state with two emission maxima at 340 nm (excitation at 315 nm) and 430 nm (excitation at 350 nm). This double luminescence has been observed previously.[5] The hybrid material, on the other hand, displays no observable luminescence. It can be reasoned, that contact between the luminescent ligand molecule and the heavy K and I atoms promotes quenching of the excited states. In order to ensure, that actual bonding between the ligand and potassium iodide, rather than their spatial proximity, leads to quenching of luminescence, the ligand L was grinded with 1 and 10 molar equivalents of KI. Both samples displayed the same luminescence as the pure ligand. Therefore, quenching of ligand's luminescence can serve as indicator of formation of the coordination network, and it will be used to study state of the hybrid material in solution (see below).

Elemental analysis. Experimental Procedure

Elemental analysis was performed on Elementar Vario ELIII analyzer at 950 ˚C with He as the carrier gas and O_2 as the combustion gas.

Elemental analysis. Results and Discussion

Elemental analysis ($C_{18}H_{16}N_6KI$): C 43.60; H 3.363; N 17.41; Calc.: C 68.34; H 5.10; N 26.56.
Crystals of the $[KI]_nL_n$ were obtained from the saturated solution of KI in MeOH. After the solvent was evaporated crystals of the desired product were manually separated from KI crystals. However it was problematic to separate main product from the fine dust which might contain extra KI and influence final EA.

Powder X-Ray Diffraction analysis (PXRD). Experimental Procedures

PXRD analysis was performed on PANalytical X´Pert Pro diffractometer with Johansson monochromator (Cu $K\alpha_1$ radiation; λ = 1.5406 Å; 45kV, 30mA). Grinded sample powder was attached to background free silicon plate using petrolatum jelly and measured with step size 0.017° on data range 3 – 100° 2θ and total measurement time of 13 hours.

Powder X-Ray Diffraction analysis (PXRD). Results and Discussion

Comparable analysis of the pattern of crystalline powder of the $[KI]_nL_n$, pattern simulated from the SXRD of KI and $[KI]_nL_n$ revealed that bulk crystalline material is containing $[K_4I_4L_4]_n$ 1D network (**Figure S3**), however KI pattern was also presented due to the reason described in the EA section.

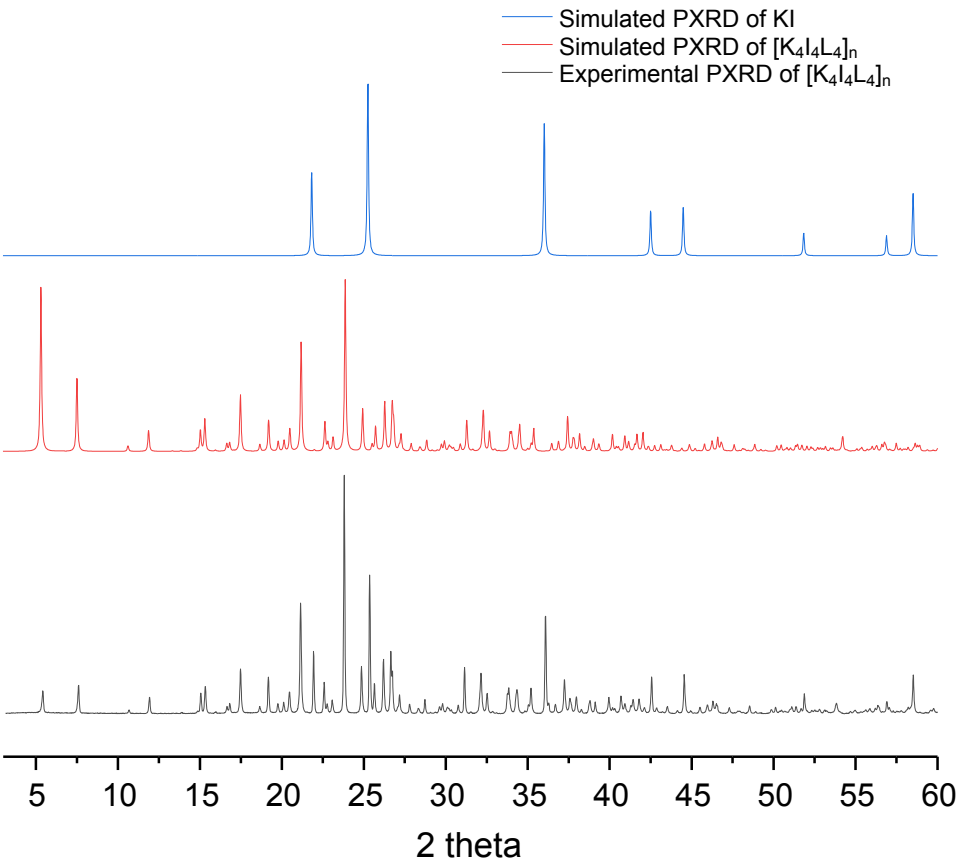

Figure S3. PXRD analysis of $[K_4I_4L_4]_n$ 1D network: black – experimental pattern of 1D network PXRD; red – simulated pattern of 1D network PXRD; blue – simulated pattern of KI PXRD.

Thermogravimetric analysis (TGA). Experimental Procedures

TGA of $[K_4I_4L_4]_n$ was performed on Perkin Elmer STA 6000 Simultaneous Thermal Analyzer with a platinum pan; sample weight was 4.997 mg. Heating scan was performed from 25 to 700 °C with a constant rate of 5 °C/min under air atmosphere (flow rate 50 ml/min).

Thermogravimetric analysis (TGA). Results and Discussion

According to thermogravimetric analysis (**Figure S4**), the polymer is stable up to temperature of ca. 200 °C, at which decomposition of the organic ligand takes place.

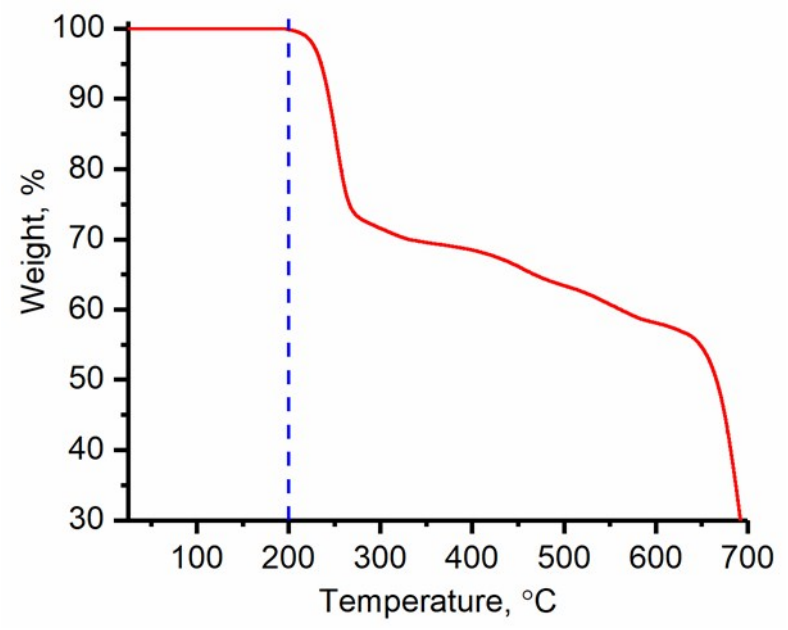

Figure S4. TGA curve of the $[K_4I_4L_4]_n$ polymer.

Liquid state studies

In order to understand, whether the coordination network remains intact or collapses upon dissolution in MeOH, liquid state studies were undertaken.

NMR spectroscopy. Experimental Procedures

^{1}H, ^{13}C, and 2D PFG ^{1}H,^{15}N HMBC NMR spectra of the ligand and its potassium complex were recorded with a Bruker Avance III 500 MHz spectrometer equipped with a 5 mm TCI Prodigy Cryoprobe operating at 500.13 MHz in ^{1}H, 125.77 MHz in ^{13}C, and 50.79 MHz in ^{15}N, respectively. The ^{1}H NMR chemical shifts were referenced to the center peak of the signal of residual CH_3OH (3.31 ppm from internal TMS), and the ^{13}C NMR chemical shifts to the center peak of the solvent CD_3OD (49.15 ppm from internal TMS). The ^{15}N chemical shifts were calibrated using CH_3NO_2 at 0.0 ppm as an external standard. A composite pulse decoupling, Waltz-16, has been used to remove proton couplings from ^{13}C NMR spectra.

NMR spectroscopy. Results and Discussion

Solution state NMR spectra of ligand (^{1}H NMR (MeOD, 500 MHz) δ, ppm: 8.30 (d, $^3J_{H\text{-}H}$ 6.10 Hz, 4H), 7.27 (s, 2H), 7.11 (s, 2H), 6.88 (d, $^3J_{H\text{-}H}$ 5.85 Hz, 4H), 5.62 (s, 4H); ^{13}C{^{1}H} NMR (MeOD, 125 MHz) δ, ppm: 150.57, 149.10, 138.89, 129.70, 124.34, 123.60, 50.57) and potassium complex (^{1}H NMR (MeOD, 500 MHz) δ, ppm: 8.33 (d, $^3J_{H\text{-}H}$ 6.05 Hz, 4H), 7.32 (d, $^3J_{H\text{-}H}$ 1.10 Hz, 2H), 7.15 (d, $^3J_{H\text{-}H}$ 1.05 Hz, 2H), 6.92 (d, $^3J_{H\text{-}H}$ 5.95 Hz, 4H), 5.65 (s, 4H); ^{13}C{^{1}H} NMR (MeOD, 125 MHz) δ, ppm: 150.53, 149.07, 138.86, 129.68, 124.35, 123.62, 50.56) show huge similarities. Solution state ^{1}H,^{15}N HMBC spectrum of the free ligand shows ^{15}N chemical shifts at δ = -210.45 ppm, δ = -120.21 ppm, and δ = -80.70 ppm. Based on the proton-nitrogen correlations the resonances at -210.45 ppm and -120.21 ppm correspond to the imidazole N-CH2 and CH=N-CH nitrogen atoms, respectively. The pyridine nitrogen atoms resonate at the chemical shift value of δ = -80.70 ppm (**Figure S5**). Addition of KI does not have notable effect on the ^{15}N chemical shifts, which with the addition of ^{1}H, ^{13}C, and 2D PFG ^{1}H,^{15}N HMBC NMR spectra similarities confirms the collapse of the complex in the liquid state.

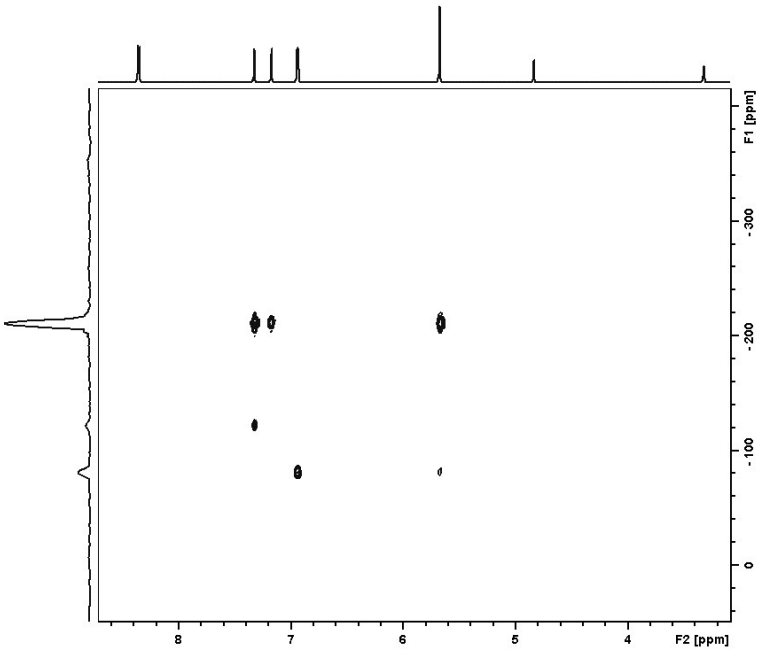

Figure S5. Solution state $^{1}H,^{15}N$ HMBC spectrum of the free ligand.

Luminescence spectroscopy. Experimental Procedures

Luminescence spectra in liquid state were recorded using Varian Cary Eclipse Fluorescence Spectrophotometer. Samples were dissolved in methanol (J.T.Baker, HPLC grade) and diluted to 50 μM concentration.

Luminescence spectroscopy. Results and Discussion

Methanol solutions of the ligand L and $[K_4I_4L_4]_n$ are both luminescent at 335 nm (excitation at 280 nm) with equal intensity. Since luminescence of the hybrid material was quenched in the solid state, this supports suggestion, that the coordination network is destroyed in solution.

Computational studies. Experimental Procedures

To understand the nature of observed interactions in solid state structure computational studies were undertaken.

All models were calculated with the Gaussian 09 program package[6] at the DFT level of theory. The hybrid density functional PBE0[7] was utilized together with the basis set consisting of the def2-TZVPPD[8] triple-zeta-valence basis set with two sets of polarization and diffuse basis functions for iodine atoms and the standard all-electron basis set 6-31G(d) for all other atoms. To study the electronic properties and interaction of the complexes, we performed topological charge density analysis with the QTAIM (Quantum Theory of Atoms in Molecules)[9] method. The analysis was done with the AIMAll program[10] using the wave functions obtained from the DFT calculations. The models for the solid state structures were directly cut from the corresponding experimental crystal structures and analyzed without geometry optimization.

Computational studies. Results and Discussion

Stabilization of the $[K_4I_4L_4]_n$ structure. The effect of the supporting ligands on the stability of the KI chain-like structure of $[K_4I_4L_4]_n$ was analyzed. Models comprising of 1, 2, and 3 $K_4I_4L_4$ units were cut directly from the crystal structure and analyzed without geometry optimization. The electron density of similar $[K_4I_4]_n$ models without supporting ligands was also analyzed and compared with the $[K_4I_4L_4]_n$ models. **Figure S6** shows a model consisting of 4 KI units and 4 ligands, and the numbering of the selected bond critical points. The calculated properties of electron density are listed in **Table S3**.

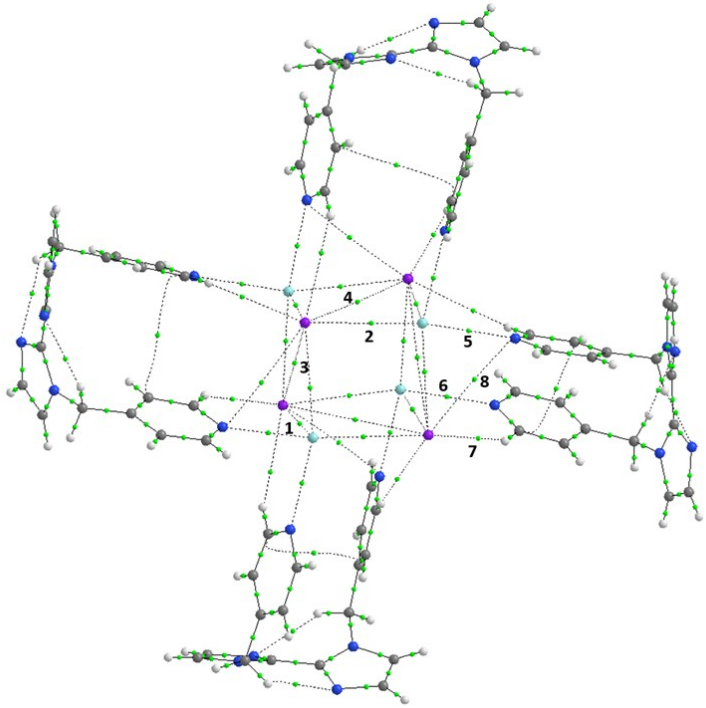

Figure S6. Bond paths (lines) and bond critical points (small green dots) in a computational model of $[K_4I_4L_4]$. The numbering of the selected bond critical points is followed in Table S3.

As can be seen, four ligands bind the potassium atoms in such a way, that a K_4I_4 "cube" is formed. In larger models, two or three of these "cubes" interact via additional K···I interactions (**Figure S7**)

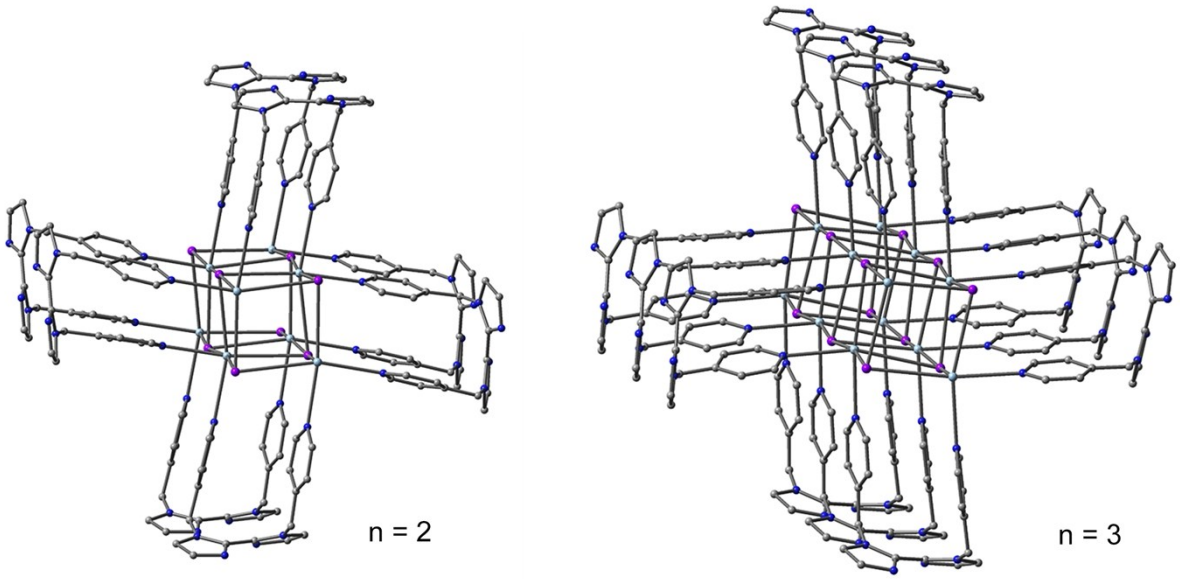

Figure S7. Models of $[K_4I_4L_4]_n$ with n = 2 and 3. Hydrogens have been removed for clarity.

In the first stage, the single-point total energies of the increasing models were calculated, and the stabilization energies were compared for $[K_4I_4]_n[K_4I_4]_{2n}$ salt (**Figure S8**, a) and ligand supported $[K_4I_4L_4]_n$ (**Figure S8**, b). The energies in both cases were referenced to the single cube, that is to the structures $[K_4I_4][K_4I_4]_2$ or $[K_4I_4L_4]$ (which therefore have a relative energy of 0).

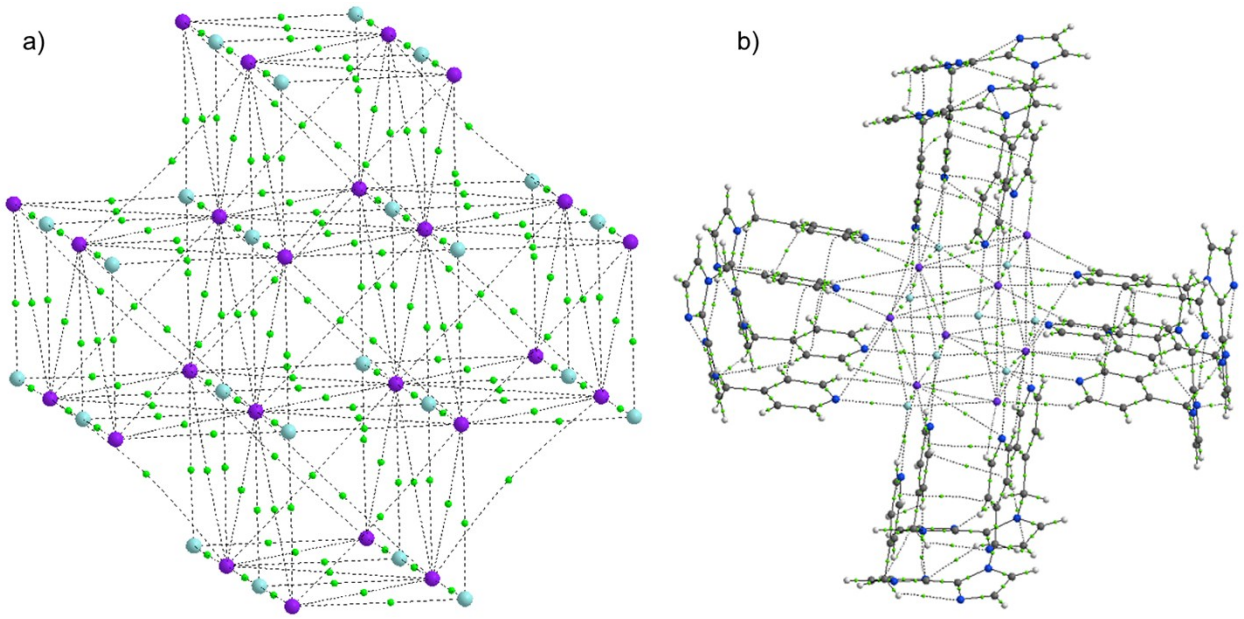

Figure S8. Models of $[K_4I_4]_n[K_4I_4]_{2n}$ salt (a) and ligand supported $[K_4I_4L_4]_n$ structure (b) with n=2 showing selected bond critical points (BCPs) and all bond paths.

Figure S9 shows the effect of the growing chain on the stabilization energies. It can be concluded, with the growth of the structure the stabilization effect of the ligands increases, because the $[K_4I_4L_4]_3$ structure with 12 ligands is about 30 kJmol^{-1} more stable compared to the $[K_4I_4]_3[K_4I_4]_6$ model without any ligands (**Table S2**). It should be noted, that with the used basis set the model $[K_4I_4L_4]_4$ had over 5700 basis functions, which made it too large for further QTAIM analysis at the DFT level of theory. The same is true to the crystal models $[K_4I_4]_n[K_4I_4]_{2n}$, which increase in size very rapidly, and, therefore, calculation of the model with n=3 as maximum was the only feasible one at the current level of theory.

Table S2. Stabilization energies [kJmol^{-1}] for the ligand supported models $[K_4I_4]_n[K_4I_4]_{2n}$ and the chain-like models $[K_4I_4]_n$ according to the number of units n. The values are referenced to the smallest n=1 unit.

n	E^{stab} $[K_4I_4]_n[K_4I_4]_{2n}$, kJmol^{-1}	E^{stab} $[K_4I_4L_4]_n$, kJmol^{-1}	Δ E^{stab} ,kJmol^{-1}
1	0	0	0
2	-131	-143	12
3	-265	-293	28

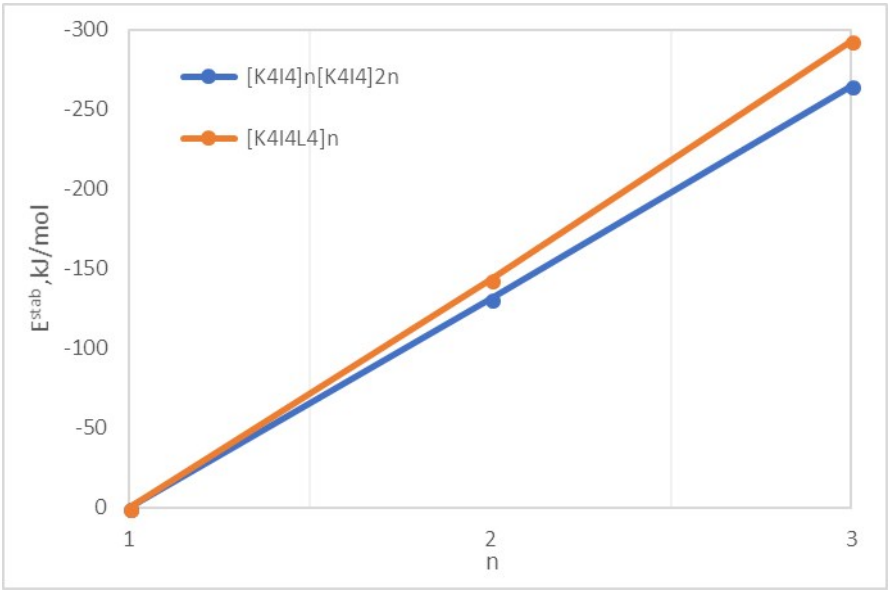

Figure S9. Effect of increasing of the model size on the stabilization energies, which are referenced to the smallest models with n=1.

Nature of the interactions. The effect of the ligands on the nature of the interactions was analyzed by QTAIM methods. Selected properties of the electron density are listed in **Table S3**, which compares the results for models $[K_4I_4]_2$, $[K_4I_4]_2[K_4I_4]_4$ and $[K_4I_4L_4]_2$. The latter model is shown in **Figure S7**, and the numbering of the selected bond critical points (BCPs) and all bond paths can be seen in a corresponding single cube model of $[K_4I_4L_4]$ in **Figure S6**. The nature of the K-I interactions is compared to single KI molecule, which was optimized with the same DFT method used to calculate all wavefunctions.

Table S3. Properties of the electron density at the selected bond critical points (BCP) according to the QTAIM analysis of the models $[K_4I_4]_2$, $[K_4I_4]_2[K_4I_4]_4$ and $[K_4I_4L_4]_2$. For numbering of the BCPs, see **Figure S6**. The selected properties are: ρ = local electron density at the BCP; |V|/G = ratio of potential energy density and kinetic energy density; δ (A,B) = delocalization index between A and B (bonding) atoms; E_{INT} = interaction energy between two interacting atoms.

BCP#	Type	ρ / *eÅ*$^{-3}$	|V|/G	δ (A,B)	E_{INT} / kJmol^{-1}
			$[K_4I_4]_2$		
1	K···I	0.063	0.81	0.11	-6.8
2	K···I	0.064	0.82	0.10	-7.0
3	I···I	0.018	0.74	0.04	-1.0
4	I···I	0.018	0.73	0.04	-1.0
			$[K_4I_4]_2[K_4I_4]_4$		
1	K···I	0.063	0.82		-6.9
2	K···I	0.062	0.81		-6.7
3	I···I	0.016	0.70		-0.9
4	I···I	0.016	0.70		-0.9
			$[K_4I_4L_4]_2$		
1	K···I	0.070	0.84	0.11	-7.8
2	K···I	0.066	0.84	0.10	-7.4
3	I···I	0.018	0.73	0.03	-1.0
4	I···I	0.018	0.73	0.03	-1.0
5	K···N	0.113	0.85		-16.4
6	K···N	0.095	0.85		-13.2
7	H···I	0.033	0.77		-4.5
8	N···I	0.033	0.85		-3.0
			KI[a]		
1	K···I	0.150	0.98	0.31	-21.7

When the $[K_4I_4]_n$ chain forms with the support of the ligands, the nature of the K···I interactions remains essentially the same than without supporting ligands, even though the interaction of the ligand nitrogen atoms with the potassium ions is fairly strong, 13-16 kJmol^{-1} (**Table S3**). All interactions are clearly electrostatic, since the ratio of potential energy density and kinetic energy density is less than 1, and only a negligible amount of electron sharing is involved, as indicated by the very small value of delocalization index, δ (A,B). The stronger K···N interactions can be suggested to further stabilize the $[K_4I_4]_n$ structure, which can be seen in the slightly larger stabilization energy of the ligand supported $[K_4I_4L_4]_n$ in the more extended models. The ligands form additional hydrogen bonding interactions as well as weak N···I interactions (**Figure S6**), which have a further role in the stabilization. Notably, the interactions remain the same even in the larger 3D models of the crystals, further indicating the electrostatic nature of the K···I interactions.

References

1 C. B. Aakeröy, J. Desper and K. W. Tharanga, *J. Mol. Struct.*, 2014, **1072**, 20–27.
2 Rikagu Oxford Diffraction, 2013.
3 L. Palatinus and G. Chapuis, *J. Appl. Crystallogr.*, 2007, **40**, 786–790.
4 G. M. Sheldrick, *Acta Crystallogr. Sect. C Struct. Chem.*, 2015, **71**, 3–8.
5 R. Tatikonda, E. Bulatov, E. Kalenius and M. Haukka, *Cryst. Growth Des.*, 2017, **17**, 5918–5926.
6 M. J. Frisch, G. W. Trucks, H. B. Schlegel, G. E. Scuseria, M. A. Robb, J. R. Cheeseman, G. Scalmani, V. Barone, B. Mennucci, G. A. Petersson, H. Nakatsuji, M. Caricato, X. Li, H. P. Hratchian, A. F. Izmaylov, J. Bloino, G. Zheng and J. L. Sonnenberg, *Inc. Wallingford, CT*, 2009.
7 J. P. Perdew, K. Burke and M. Ernzerhof, *Phys. Rev. Lett.*, 1997, 78, 1396.
8 D. Rappoport and F. Furche, *J. Chem. Phys.*,2010, **133**, 134105.
9 R. F. W. Bader, *Atoms in Molecules: A Quantum Theory*, 1990.
10 T. A. Keith, *TK Gristmill Software, Overl. Park KS, USA*, 2003.

Author Contributions

Margarita Bulatova – synthesis, data analysis, writing original draft;

Pipsa Hirva – computational studies;

Evgeny Bulatov – luminescence spectroscopy, PXRD experiment, TGA;

Rajendhraprasad Tatikonda – SXRD experiment;

Elina Sievänen – NMR experiments;

Matti Haukka – Project leader, crystallography.